

Osteoarthritis and Cartilage



Cell and matrix morphology in articular cartilage from adult human knee and ankle joints suggests depth-associated adaptations to biomechanical and anatomical roles



T.M. Quinn †, H.-J. Häuselmann ‡, N. Shintani †, E.B. Hunziker †*

† Center of Regenerative Medicine for Skeletal Tissues, Departments of Osteoporosis, Orthopaedic Surgery and Clinical Research, University of Bern, Bern, Switzerland

‡ Zentrum für Rheuma - und Knochenerkrankungen, Klinik im Park, Zürich, Switzerland

ARTICLE INFO

Article history:

Received 10 June 2013

Accepted 24 September 2013

Keywords:

Human
Knee
Ankle
Articular cartilage
Morphology

SUMMARY

Objective: Marked differences exist between human knee and ankle joints regarding risks and progression of osteoarthritis (OA). Pathomechanisms of degenerative joint disease may therefore differ in these joints, due to differences in tissue structure and function. Focusing on structural issues, which are design goals for tissue engineering, we compared cell and matrix morphologies in different anatomical sites of adult human knee and ankle joints.

Methods: Osteochondral explants were acquired from knee and ankle joints of deceased persons aged 20–40 years and analyzed for cell, matrix and tissue morphology using confocal and electron microscopy (EM) and unbiased stereological methods. Morphological variations disclosing an association between joint type (knee vs ankle) and biomechanical role (convex vs concave articular surfaces) were identified by a 2-way analysis of variance (ANOVA) and a post-hoc analysis.

Results: Knee cartilage exhibited higher cell densities in the superficial zone than ankle cartilage. In the transitional zone, higher cell densities were observed in association with convex vs concave articular surfaces, without significant differences between knee and ankle cartilage. Highly uniform cell and matrix morphologies were evident throughout the radial zone in the knee and ankle, regardless of tissue biomechanical role. Throughout the knee and ankle cartilage sampled, chondron density was remarkably constant at approximately 4.2×10^6 chondrons/cm³.

Conclusion: Variation in cartilage cell and matrix morphologies with changing joint and biomechanical environments suggests that tissue structural adaptations are performed primarily by the superficial and transitional zones. Data may aid the development of site-specific cartilage tissue engineering, and help to identify conditions where OA is likely to occur.

© 2013 Published by Elsevier Ltd on behalf of Osteoarthritis Research Society International.

Introduction

Articular cartilage microstructural organization is intimately related to cell metabolism and tissue biomechanical function. Cartilage exhibits functional zones correlated with depth from the articular surface, referred to as the superficial, transitional and deep zones. The superficial zone includes approximately the first 10% of

tissue immediately under the articular surface and is characterized by collagen fibers oriented parallel to the articular surface, relatively low proteoglycan density and flattened, individual chondrocytes¹. The transitional zone includes the next 10% of tissue; it exhibits more isotropically oriented collagen fibers and more rounded, individual chondrocytes. The radial zone extends the rest of the way through the tissue to the interface with underlying subchondral bone; its structural hallmarks include collagen fibers oriented perpendicular to the articular surface and chondrocytes grouped into multicellular columnar structures termed chondrons^{1,2}. Within each zone, chondrocytes continually turn over and remodel non-fibrillar collagens as well as the non-collagenous portion of the locally specialized extracellular matrix in response to the biomechanical demands of joint loading^{3–5}. In the vicinity of individual cells, the extracellular matrix is further organized into an

* Address correspondence and reprint requests to: E.B. Hunziker, Center of Regenerative Medicine for Skeletal Tissues, Departments of Osteoporosis, Orthopaedic Surgery and Clinical Research, University of Bern, Murtenstrasse 35, P.O. Box 54, 3010 Bern, Switzerland. Tel: 41-31-632-86-85; Fax: 41-31-632-49-55.

E-mail addresses: thomas.quinn@mcgill.ca (T.M. Quinn), hjhauselmann@rheumazentrum.ch (H.-J. Häuselmann), nahoko.shintani@dkf.unibe.ch (N. Shintani), ernst.hunziker@dkf.unibe.ch (E.B. Hunziker).

immediately pericellular zone and an interterritorial matrix between cells. The pericellular matrix is rich in proteoglycans⁶, possesses a particular collagen composition and architecture and forms a thin layer around the associated chondrocyte; it appears to play an important role in mechanotransduction and metabolism of that particular cell⁷. The interterritorial matrix forms the bulk of cartilage extracellular matrix and provides structural and biomechanical contiguity between cells and throughout the tissue. Structural organization within these depth-associated tissue zones and cell-associated matrices must be consistent with the multiple concurrent demands of local metabolism and biomechanics for long-term tissue function; therefore they represent important design goals from the point of view of cartilage tissue engineering.

Structural differences in cartilage tissue from different synovial joints provide important insights into how the tissue fulfills its biomechanical role in disparate anatomical contexts⁸. Of special interest are differences between cartilage in the adult human knee and ankle, since both of these joints of the lower limb participate actively in locomotion yet exhibit marked differences in the prevalence and progression of degradative joint disease^{9–14}. The human knee joint provides for articulation between the distal femur and tibial plateau, and is a relatively common site of sports injury and osteoarthritis (OA)¹¹. The progression of post-traumatic OA in the knee appears to be more rapid than in the ankle⁹, resulting in generalized changes in locomotor function^{13,15}. The human ankle joint, or talocrural joint between the distal tibia (DTB) and fibula and the talus, is a hinge joint with highly congruent articulating surfaces which is less often afflicted with symptomatic OA¹¹. Interactions between the two joints with respect to altered biomechanics and degradative disease have been clearly established^{14–18}, but nevertheless the knee is markedly more prone to develop OA than the ankle⁹. Contributing factors to these differences in the prevalence and presentation of OA between the knee and ankle may include differences in cartilage thickness¹⁹, cell density and metabolic rates^{20,21} and material properties²². More thorough characterization of factors which contribute to OA but differ between knee and ankle cartilage, including cell and matrix morphologies which reflect the cell-scale metabolic and biophysical environment, would therefore provide valuable insights into the etiology and progression of OA^{21,23,24}.

The prevalence of OA in particular joint locations associated with relatively strenuous mechanical loading^{12,25,26} suggests that particularities of the local loading environment are important to tissue pathology, and may have important influences on cartilage cell and matrix morphologies even under normal physiological conditions. Previous studies suggest that different anatomical locations within the adult human knee might be associated on the basis of similar cartilage cell and matrix morphologies²⁷. These groupings may in part represent cartilage adaptations to specific biomechanical roles. In the knee, the femoral condyles function as convex surfaces with moving points of contact, while the tibial plateau functions as a concave surface with relatively constant contact points²⁸. Morphologic differences in cartilage between the condyles and the tibial plateau²⁷ may therefore reflect structural adaptations to these distinct roles. If so, then similar differences may appear elsewhere in the body such as in the ankle joint where the talar dome (TAL) rotates relative to the DTB. The identification of relationships between cartilage cell and matrix morphologies and specific biomechanical roles would be of significant interest for a better understanding of cartilage physiology and cell-scale biomechanics.

Our goals were to quantify and compare cell and matrix morphologies in articular cartilage obtained from four well-defined locations in adult human knee and ankle joints. Comparisons were made both in terms of the joint from which cartilage samples

were acquired (knee vs ankle) and in terms of the articular biomechanical role played by the cartilage surfaces from which samples were acquired (convex vs concave). Unbiased stereological estimators of cell and matrix morphology were used to acquire quantitative data for statistical analysis, with attention to differences within depth-associated tissue zones and cell-associated pericellular and interterritorial matrix morphologies. Information obtained provides valuable reference data for insights into relationships between tissue structure, biomechanics and remodeling, and for identification of design goals for cartilage tissue engineering.

Methods

With approval from the Medical Ethics Commission and the cooperation of the University of Bern's Department of Forensic Medicine, articular cartilage samples were obtained from 10 adult humans (nine men aged 20–40 years and one woman aged 23 years) as previously described^{2,27}. Subjects were victims of traffic accidents, suicide or drug overdose and had suffered from neither acute nor chronic disease. Tissue was removed within 48 h of death; all knee and ankle joints exhibited healthy articular surfaces. 2–3 cylindrical osteochondral explants of 4 mm diameter were drilled perpendicular to the articular surface from four locations in the knee and ankle: the medial femoral condyle (MFC), the portion of the medial tibial plateau not covered by meniscus (MTN), the TAL and the DTB. Precise definition of locations was limited by restrictions related to anatomical dissecting and the need to reconstitute the joint. Nevertheless, locations were defined with similar precision to previous studies^{19,29–31}. Concerns relating to joint reconstitution also resulted in only eight of the donors providing knee cartilage, while all 10 provided ankle cartilage.

Immediately after biopsy, tissue cylinders were fixed in 5% glutaraldehyde (buffered with 0.1 M sodium cacodylate, pH 7.4) over 1 week at ambient temperature. This fixation protocol results in autofluorescence, which improves cell contrast during confocal microscopy. Explants were then stored in 70% ethanol at 4°C (typically for a few days); this protocol has been shown to induce negligible deformation artifacts² [Fig. 1].

Details of confocal microscope sample preparation are shown in the [Supplementary Data section](#). A laser scanning confocal microscope (MRC 600 LSC imaging system; Bio-Rad, Hertfordshire, UK) was used at a zoom of 1 with a 60× oil-immersion objective (numerical aperture 1.4), an argon laser excitation source (488 nm) with a 510 nm longpass emission filter. Under light microscopy, the thickness of hyaline articular cartilage from the articular surface to the tidemark was measured and used to define three tissue zones: superficial (10% of thickness), transitional (10%), and radial (80%). The radial zone was further divided into four sub-zones (each 20% of tissue thickness). Within each tissue zone, stereological dissectors were obtained in the form of serial optical sections (confocal images covering an area of 180 × 240 μm²) spaced 5 μm apart (at increasing depth of focus into the specimen). Four sequential scans were averaged to acquire a single image. These were photographed using color slide film and projected to a final magnification of 870× for stereological measurements. Two images were acquired per dissector in the superficial and transitional zones, and four images were acquired per dissector in each radial zone. Thicker dissectors were used for the radial zone because these were more suitable for a stereological analysis of chondrons, which are larger than chondrocytes.

Established stereological methods^{32,33} were used for estimation of four primary morphological parameters from confocal images: chondrocyte volume per unit tissue volume (V_V), cell surface area per unit tissue volume (S_V), and number of cells and chondrons per

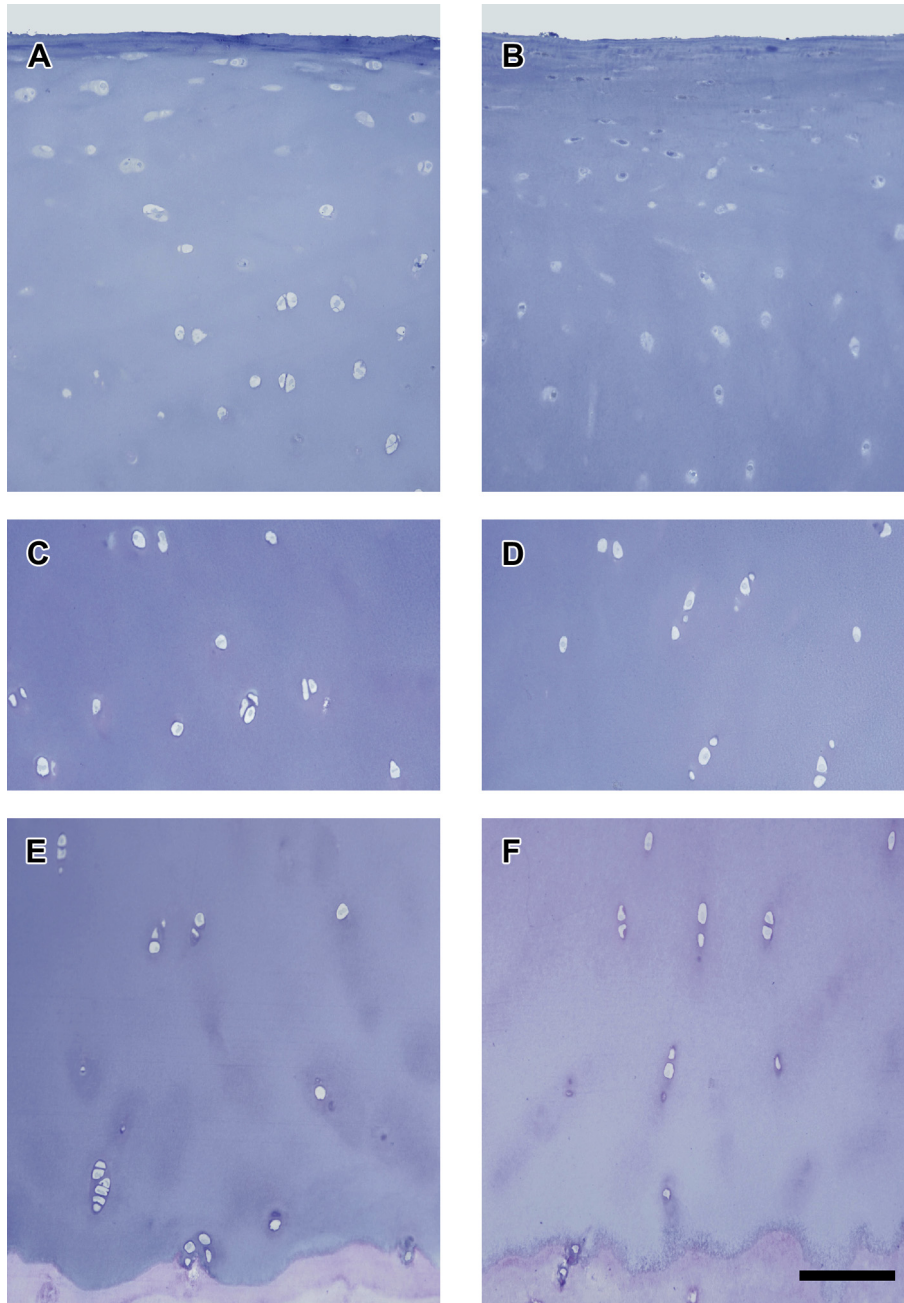


Fig. 1. Light micrographs of normal adult human articular cartilage originating from the superficial/transitional zones (A: talar dome, B: medial tibial plateau), the upper radial zone (C: talar dome, D: medial tibial plateau), and the lower radial zone (E: talar dome, F: medial tibial plateau). In the superficial zone, chondrocytes are relatively flattened with elliptical profiles. In the transitional zone, chondrocytes are more rounded, and in the radial zone they tend to be grouped in vertical stacks (chondrons). Semi-thin (1 μm thick) sections of Epon-embedded tissue stained with Toluidine Blue O. Bar = 100 μm .

unit tissue volume (N_V and N_{Vc}). For V_V , a 10×10 grid of points was placed over a single projected image, and the number of points “touching” cells was counted. This number (expressed as percent) provided an estimator of V_V . For S_V , a rectangular 6×6 grid of cycloid arcs was placed over a projected image, and the number of intersections (I) with cell-matrix interfaces was counted. Then S_V was estimated as $2 \times I/L^{34}$, where $L = 1.82$ mm was the total length of cycloid arcs in “image-space”. N_V and N_{Vc} were estimated as numbers of cells or chondrons, respectively, which did not appear in the first image of a dissector, but which appeared in subsequent images, divided by the dissector volume. The dissector surface used for determining N_V and N_{Vc} was delimited by a $134 \times 178 \mu\text{m}^2$ bounding box. This was deliberately chosen to be smaller than the

$180 \times 240 \mu\text{m}^2$ images to allow for the consistent allocation of cells to rectangular blocks of tissue in 3-D space: only cells or chondrons which appeared within the bounding box but did not touch its lower or left boundaries were included.

Five secondary parameters were then estimated including characteristic cell volume ($V = V_V/N_V$), cell surface area ($S = S_V/N_V$), matrix volume per cell ($M = 1/N_V - V$), number of cells per chondron ($N_c = N_V/N_{Vc}$), and matrix volume per chondron ($M_c = 1/N_{Vc} - N_c \times V$). For comparison to “Stockwell’s rule”³⁵, the total number of cells per unit articular surface (N_{AS}) was determined as the sum of $N_V \times d$ over all of the six tissue zones, where d represents zone thickness. Similarly, the total number of chondrons per unit articular surface (N_{ASc}) was also determined.

A subset of explants from MTN and TAL cartilage was also prepared for electron microscopy (EM) imaging (details of EM sample preparation are shown in the [Supplementary Data section](#)). EM images were acquired on a Hitachi H-7000B electron microscope at 2000 \times magnification [Fig. 2]; systematically random sampled images were printed at a final magnification of 4000 \times . Printed EM images were used to estimate the volume of pericellular matrix per total matrix volume (P_M) [Figure S1 in Supplementary Data]. A 10×10 grid of points was placed over each projected image while the numbers of points “touching” pericellular or any extracellular

matrix were counted; these numbers directly provided estimates of pericellular matrix and extracellular matrix volume fractions (in units of percent). P_M was then estimated by the ratio of pericellular to extracellular matrix volume fractions. P_M was also combined with the volume of matrix per cell (M) determined from confocal microscope stereology for determination of pericellular and interterritorial matrix volumes per cell.

Data were averaged over 8 (knee) or 10 (ankle) human specimens. Variations in morphological parameters between the four distinct anatomical locations were examined by 2-way analysis of

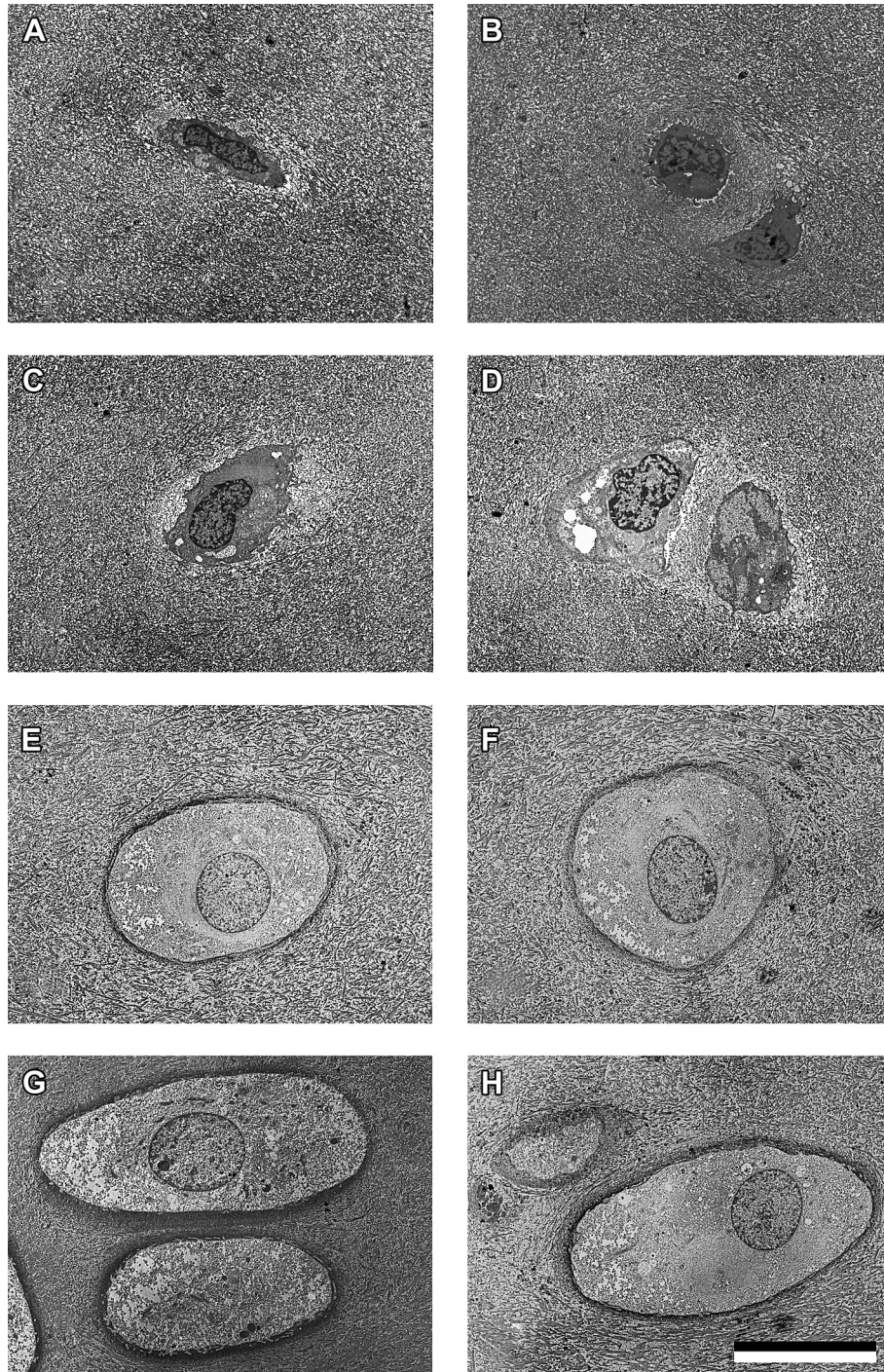


Fig. 2. Transmission electron micrographs of normal adult human articular cartilage originating from the superficial zone (A: talar dome, B: medial tibial plateau), the transitional zone (C: talar dome, D: medial tibial plateau), the upper radial zone (E: talar dome, F: medial tibial plateau) and the lower radial zone (G: talar dome, H: medial tibial plateau). Thin (60 nm thick) sections of Epon-embedded tissue stained with uranyl acetate and lead citrate. Bar = 10 μ m.

variance (ANOVA) with post-hoc Tukey tests; results were considered significant for $P < 0.05$. Axes of the ANOVA were defined by grouping anatomical locations in terms of the joint involved and in terms of the biomechanical role played by articulating surfaces within the joint. Therefore, knee cartilage was compared to ankle cartilage (MFC + MTN vs TAL + DTB) while convex articular surfaces were compared to concave surfaces (MFC + TAL vs MTN + DTB). Differences in pericellular or interterritorial matrix volumes per cell between depth-associated zones in MTN vs TAL cartilage were assessed by Student's *t*-test. Data are presented as mean \pm 95% confidence limits (*n*).

Results

Articular cartilage thickness measurements [Fig. 3] were consistent with previous findings¹⁹. Thickness varied somewhat within the knee (2.4 ± 0.4 mm at the MFC and 3.0 ± 0.4 mm at the MTN) but considerably less within the ankle (1.6 ± 0.2 mm at the TAL and 1.5 ± 0.2 mm at the DTB). Ankle cartilage was significantly thinner than knee cartilage, but no significant differences associated with biomechanical role (convex vs concave) were observed [Fig. 3].

In the superficial zone, cell densities appeared to be generally higher than in the deeper tissue zones for anatomical sites within the knee, as expected^{1,2,27}. However, elevated cell density was not evident in the superficial zone of ankle cartilage [Table I; Fig. 4]. As a consequence, morphological parameters relating to cell density in the superficial zone including cell volume fraction (V_V), cell surface area per unit volume (S_V) and cell number density (N_V) were significantly greater in knee vs ankle cartilage [Table I; Fig. 4(a)]. Matrix volume per cell (M) in the superficial zone was correspondingly significantly less in knee vs ankle cartilage [Table I]. No significant differences in cell and matrix morphological parameters associated with the articular biomechanical role of the source cartilage (convex vs concave surfaces) were observed in superficial zone cartilage.

In the transitional zone, no significant differences in cell and matrix morphological parameters associated with the joint from which cartilage samples were acquired (knee vs ankle) were observed. However, significant effects associated with articular biomechanics were evident [Table I; Fig. 4(b)]. Cartilage acquired from convex articular surfaces (MFC and TAL) exhibited significantly higher cell volume fraction (V_V) and cell surface area per unit volume (S_V) in the transitional zone, as compared to tissue acquired from concave surfaces (MTN and DTB).

As in previous studies^{2,27}, preliminary statistical analyses indicated negligible variations in cell and matrix morphological parameters between the four different radial sub-zones. Therefore, for each anatomical site, data which had been sampled from the four radial sub-zones were pooled into a single zone representing the

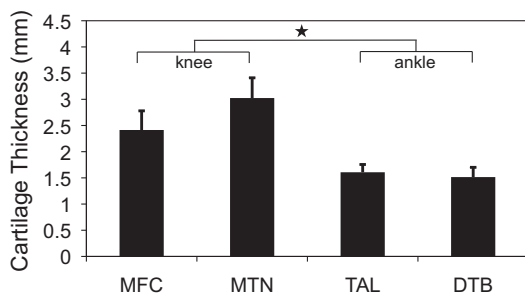


Fig. 3. Cartilage thickness at four different anatomical sites in the human knee (MFC and MTN) and ankle (TAL and DTB; mean \pm 95% confidence limits, $n = 10$). Star (*) indicates significantly different thicknesses between knee vs ankle cartilage ($P < 0.05$).

deepest 80% of the cartilage layer. In the radial zone, no significant differences in cell and matrix morphological parameters were observed, regardless of whether data were examined as a function of the joint from which cartilage samples were acquired (knee vs ankle) or as a function of articular biomechanics [convex vs concave joint surfaces; Fig. 4(c)]. Neither were significant differences observed among chondron morphological parameters [Table II]. (Multiple-cell chondrons were observed only in the radial zone, therefore chondron morphological parameters were identical to cell morphological parameters in the superficial and transitional zones.)

When data were averaged over the full tissue depth [Table III], significant differences in primary cell and matrix morphological parameters remained where they had previously been seen regarding articular biomechanics-related effects in the transitional zone [Table I]. Specifically, tissue-average cell volume density [V_V ; Table III] was significantly greater in convex vs concave articular surfaces. Effects associated with differences between joints were also observed: the total numbers of cells and chondrons per unit articular surface (N_{AS} and N_{ASC} respectively) were significantly greater in knee vs ankle cartilage.

Pericellular matrix volume per total matrix volume (P_M) did not vary significantly between MTN and TAL cartilage, for any depth-associated tissue zone. P_M was $9.1 \pm 3.5\%$ and $9.6 \pm 1.9\%$ in MTN and TAL superficial zone, $7.4 \pm 2.1\%$ and $10.5 \pm 3.5\%$ in MTN and TAL transitional zone, and $10.1 \pm 1.8\%$ and $9.3 \pm 2.2\%$ in MTN and TAL radial zone. Pericellular matrix volume per cell appeared to increase slightly with depth in MTN tissue, being 9.6 ± 5.0 , 10.5 ± 5.8 and $15.9 \pm 6.3 \times 10^3 \mu\text{m}^3$ in superficial, transitional and radial zone tissue, respectively [Fig. 5(a)]. The same trend did not appear to be as strong in TAL tissue, where pericellular matrix volume per cell was 10.5 ± 4.7 , 12.0 ± 6.1 and $12.7 \pm 3.7 \times 10^3 \mu\text{m}^3$ in superficial, transitional and radial zones [Fig. 5(b)]. However, within any zone, no statistically significant differences between MTN and TAL cartilage were detected with respect to pericellular or interterritorial matrix volumes per cell [Fig. 5].

Discussion

Significant differences between articular cartilage taken from adult human knees vs ankles were readily observed in terms of relatively thin ankle cartilage [Fig. 2], consistent with previous findings¹⁹. However, at the level of cell and matrix morphologies, joint-associated differences were largely limited to the tissue superficial zone. Cartilage throughout adult human knees (with the exception of the patellar groove²⁷) tends to exhibit relatively high cell densities in the superficial zone as compared to the transitional and radial (deep) zones of the tissue. In contrast, for ankle cartilage taken from both the TAL and the DTB, cell densities were found to be very similar between the superficial and deep zones [Table I]. This suggests that the superficial zone of adult human ankle cartilage is not as distinctive an anatomical entity as it is in knee cartilage, at least not in terms of the cell-based morphological parameters examined in the present study. That the morphology of the superficial zone is strongly associated with the joint within which articulation occurs is perhaps not surprising. The biomechanical solicitation of cartilage in terms of interstitial fluid flows and mechanical deformations is greatest in the superficial zone, where exchange with the synovial fluid occurs most readily. Therefore it seems reasonable that different joints within the body would place markedly different demands on cartilage superficial zone function (and hence structure), due to differences in compressive and shear loading patterns, congruence between the articular surface and the underlying bone^{19,36}, and other factors arising from joint geometry and biomechanics^{37,38}.

Table I

Summary of results for cell and matrix morphological parameters measured within the superficial, transitional, and radial (deep) zones of cartilage from four different locations in the adult human knee and ankle (mean \pm 95% confidence limits)

	V_V (%)	S_V (mm^{-1})	N_V (10^3 mm^{-3})	V (μm^3)	S (μm^2)	M ($10^3 \mu\text{m}^3$)	n
Superficial Zone							
MFC	2.6 \pm 0.7 ^k	15.0 \pm 2.7 ^k	24.0 \pm 7.5 ^k	1,240 \pm 560	670 \pm 130	46 \pm 14 ^k	8
MTN	1.7 \pm 0.6 ^k	9.1 \pm 2.5 ^k	13.8 \pm 2.9 ^k	1,200 \pm 480	650 \pm 140	76 \pm 18 ^k	8
TAL	1.4 \pm 0.6 ^a	6.7 \pm 2.0 ^a	10.0 \pm 2.4 ^a	1,420 \pm 490	660 \pm 100	107 \pm 29 ^a	10
DTB	1.3 \pm 0.6 ^a	7.9 \pm 2.0 ^a	10.7 \pm 2.4 ^a	1,300 \pm 600	800 \pm 210	102 \pm 26 ^a	10
Transitional Zone							
MFC	2.1 \pm 0.5 ^x	9.0 \pm 1.5 ^x	10.3 \pm 1.1	2,090 \pm 520	880 \pm 130	97 \pm 12	8
MTN	1.3 \pm 0.7 ^c	5.7 \pm 1.8 ^c	9.0 \pm 2.3	1,590 \pm 960	690 \pm 310	119 \pm 29	8
TAL	2.2 \pm 0.4 ^x	8.0 \pm 1.6 ^x	10.9 \pm 2.6	2,250 \pm 790	820 \pm 290	100 \pm 26	10
DTB	1.7 \pm 0.5 ^c	7.3 \pm 1.8 ^c	10.0 \pm 2.7	1,790 \pm 620	760 \pm 160	115 \pm 39	10
Radial Zone							
MFC	1.5 \pm 0.7	6.8 \pm 2.1	7.7 \pm 2.0	2,020 \pm 1,020	910 \pm 330	141 \pm 41	8
MTN	1.1 \pm 0.6	5.2 \pm 2.2	7.1 \pm 2.1	1,530 \pm 690	730 \pm 210	148 \pm 40	8
TAL	1.4 \pm 0.5	5.5 \pm 1.6	7.6 \pm 1.3	1,850 \pm 690	730 \pm 190	137 \pm 26	10
DTB	1.4 \pm 0.5	6.3 \pm 1.8	7.6 \pm 1.7	1,820 \pm 660	830 \pm 200	143 \pm 35	10

MFC = medial femoral condyle; MTN = medial tibial plateau (not meniscus-covered); TAL = talar dome; DTB = distal tibia; V_V = chondrocyte volume per unit cartilage volume; S_V = chondrocyte surface area per unit cartilage volume; N_V = number of chondrocytes per unit cartilage volume; V = chondrocyte volume; S = chondrocyte surface area; M = matrix volume per chondrocyte. Statistical comparisons were calculated between locations (not between tissue zones). Within the data set for each morphological parameter, the letters "k" and "a" indicate a significant difference related to the joint from which samples were taken (knee vs ankle), while the letters "x" and "c" indicate a significant difference related to the biomechanical role played by apposing joint surfaces (convex vs concave).

One factor relating to joint biomechanics, which was emphasized in the present study, was the distinction between convex and concave articular surfaces. Interestingly, effects associated with this biomechanical distinction were the most evident in the transitional zone [Table I], where cell volumes per unit volume (V_V) and cell surface areas per unit volume (S_V) were consistently higher in

cartilage from convex vs concave articular surfaces. The transitional zone plays an important biomechanical role during shear of articular cartilage³⁹, and may represent the region of minimum shear modulus and maximum shear strain⁴⁰. It is therefore possible that our grouping of samples based upon articular biomechanics may have highlighted specific functional adaptations to tissue shear loading, which are emphasized in the transitional zone. The observed differences in cell and matrix morphological parameters in the transitional zone associated with articular biomechanics were among the stronger effects observed in the present study, since they were preserved even when data were considered as tissue-averages [Table III].

In addition to the differences observed in association with the joint (knee vs ankle) and in association with articular biomechanics (convex vs concave joint surfaces), several of the measured cell and matrix morphological parameters were highly consistent throughout this study. Chondrocyte volumes (V) and surface areas (S) did not show any variation under any of the analyses performed, and did not appear to vary strongly between tissue zones either [Tables I and III]. This suggests that basic aspects of chondrocyte morphology are highly conserved for cartilage throughout the adult human knee and ankle. In the radial (deep) zone, no differences were observed in any cell, matrix, or chondron morphological parameters [Tables I and II], indicating that the radial zone, in contrast to the superficial and transitional zones, is a highly conserved structure throughout the human knee and ankle. This suggests that structural adaptation of cartilage due to specific joint biomechanical environments may be primarily achieved by modifications in the superficial and transitional zones, while the radial zone is relatively invariant. The tissue-averaged number of cells per

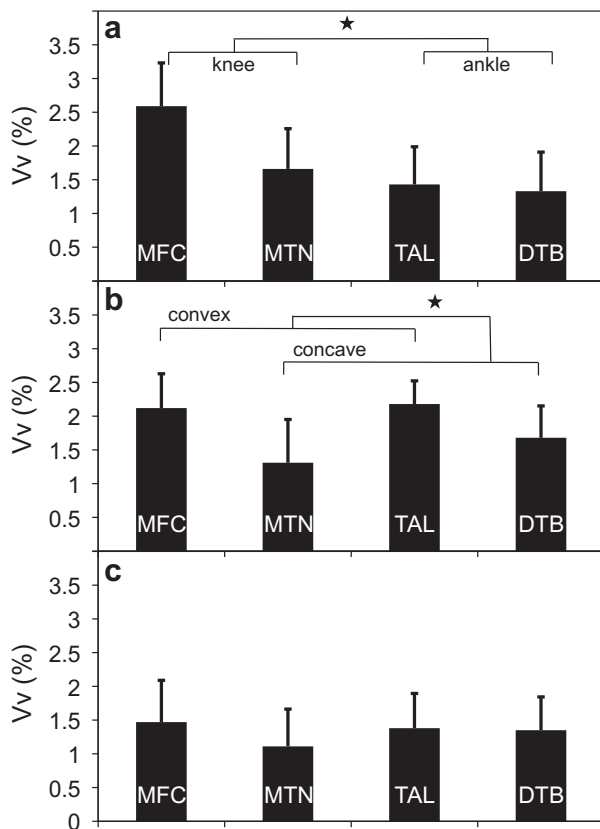


Fig. 4. Cell volume per unit tissue volume (V_V) within cartilage from four different anatomical sites in the human knee (MFC and MTN; mean \pm 95% confidence limits, $n = 8$) and ankle (TAL and DTB; $n = 10$). Data were acquired from confocal microscopy of a) superficial zone, b) transitional zone, and c) radial zone cartilage. Star (★) indicates significant differences in V_V between knee vs ankle cartilage, or between cartilage from convex (MFC and TAL) vs concave (MTN and DTB) articular surfaces ($P < 0.05$).

Table II

Summary of results for chondron and matrix morphological parameters measured within the radial (deep) zone of cartilage from four different locations in the adult human knee and ankle (mean \pm 95% confidence limits)

	N_c	N_{Vc} (10^3 mm^{-3})	M_c ($10^3 \mu\text{m}^3$)	n
MFC	6.3 \pm 4.5	1.7 \pm 0.9	780 \pm 490	8
MTN	3.6 \pm 1.8	2.3 \pm 0.9	520 \pm 230	8
TAL	3.4 \pm 1.3	2.6 \pm 0.6	450 \pm 160	10
DTB	3.1 \pm 1.2	2.8 \pm 0.8	420 \pm 170	10

See Table I for definitions of locations (MFC, MTN, TAL, DTB). N_c = number of chondrocytes per chondron; N_{Vc} = number of chondrons per unit cartilage volume; M_c = matrix volume per chondron. No significant differences between locations were detected in these data.

Table III

Summary of results for tissue-average cell, chondron, and matrix morphological parameters measured within cartilage from four different locations in the adult human knee and ankle (mean \pm 95% confidence limits)

	V_V (%)	S_V (mm^{-1})	N_V (10^3 mm^{-3})	V (μm^3)	S (μm^2)	M ($10^3 \mu\text{m}^3$)	N_{AS} (10^3 mm^{-2})	n
MFC	1.7 ± 0.4^x	7.8 ± 1.3	9.6 ± 1.2	$1,750 \pm 450$	820 ± 160	104 ± 12	23.7 ± 4.3^k	8
MTN	1.2 ± 0.2^c	5.6 ± 0.8	7.9 ± 0.9	$1,480 \pm 190$	710 ± 60	126 ± 15	24.2 ± 4.3^k	8
TAL	1.5 ± 0.2^x	5.9 ± 0.5	8.2 ± 0.7	$1,810 \pm 210$	730 ± 60	122 ± 10	13.2 ± 1.9^a	10
DTB	1.4 ± 0.3^c	6.5 ± 1.2	8.2 ± 1.1	$1,680 \pm 290$	800 ± 110	125 ± 17	12.2 ± 1.6^a	10
	N_c	N_{Vc} (10^3 mm^{-3})	M_c ($10^3 \mu\text{m}^3$)	N_{Asc} (10^3 mm^{-2})	n			
MFC	2.1 ± 0.4	4.8 ± 1.1	218 ± 49	11.6 ± 2.3^k	8			
MTN	2.0 ± 0.3	4.1 ± 0.8	251 ± 42	12.8 ± 3.9^k	8			
TAL	2.0 ± 0.2	4.2 ± 0.6	245 ± 33	6.8 ± 1.4^a	10			
DTB	1.9 ± 0.2	4.3 ± 0.6	238 ± 39	6.4 ± 0.4^a	10			

See Table I for definitions of locations (MFC, MTN, TAL, DTB) and morphological parameters (V_V , S_V , N_V , V , S , M , N_c , N_{Vc} , M_c). N_{AS} = total number of chondrocytes per unit articular surface; N_{Asc} = total number of chondrons per unit articular surface. Statistical comparisons were calculated between locations (not between tissue zones). Within the data set for each morphological parameter, the letters "k" and "a" indicate a significant difference related to the joint from which samples were taken (knee vs ankle), while the letters "x" and "c" indicate a significant difference related to the biomechanical role played by apposing joint surfaces (convex vs concave).

chondron (N_c) also showed no significant variation, at a typical value of 2.0 [Table III]. Tissue-averaged number of chondrons per unit volume (N_{Vc}) and matrix volume per chondron (M_c) also showed no variation around characteristic values of 4.4×10^6 chondrons per cm^3 and $238,000 \mu\text{m}^3$, respectively. Pericellular matrix volume fraction P_M was limited to the range 7.4–10.5% throughout all depth-associated tissue zones, and showed no significant difference between medial tibia and TAL cartilage. Combination of stereological data from confocal and EM allowed for quantification of pericellular and interterritorial matrix volumes per cell in MTN and TAL cartilage [Fig. 5]; however, no statistically significant differences in these cell-matrix morphological parameters were detected between these anatomical locations, for any depth within the tissue. Notably, "Stockwell's rule"³⁵, which suggests that the numbers of chondrocytes or chondrons beneath a unit area of articular surface (N_{AS} or N_{Asc}) are relatively constant, was not supported by the present data; both parameters showed significant variations in knee vs ankle comparisons [Table III]. This was consistent with the significantly greater thickness of knee vs ankle cartilage [Fig. 2] combined with the relatively small (or no) observed variation in tissue-averaged cell and chondron densities [Table III].

An important source of error in the present study was associated with the limitations of defining tissue zones according to proportional thicknesses, rather than according to cell morphology and matrix composition. This was done to establish a repeatable experimental procedure, and to avoid the ambiguity of identifying locations of zonal boundaries. However, this limitation indicates that new morphometric methods such as three-dimensional cartilage imaging⁴¹ could be used in the future to qualify and amplify present findings. It should also be recognized that it is difficult to separate effects associated with the joint (knee vs ankle) from effects relating to joint biomechanics (convex vs concave articular surfaces). Different synovial joints, such as the human knee and ankle, can have very different anatomical shapes, mechanisms of stabilization and roles in the locomotor apparatus. Therefore while it seems reasonable to identify relatively obvious biomechanical roles for joint surfaces (such as convex vs concave joint surfaces as was done in the present study), it is almost certainly the case that comparisons which follow are confounded by additional variables relating to joint loading geometries, waveforms, force magnitudes and other factors.

Contributions

Conception and design: EBH.

Analysis and interpretation of the data: TMQ, HJH, NS, EBH.

Drafting of the article: TMQ.

Critical revision of the article for important intellectual content: HJH, NS, EBH.

Final approval of the article: TMQ, HJH, NS, EBH.

Provision of study materials or patients: HJH, EBH.

Statistical expertise: TMQ.

Obtaining of funding: EBH.

Administrative, technical, or logistic support: TMQ, HJH, EBH.

Collection and assembly of data: TMQ, NS, EBH.

Competing interests

The authors have no conflicts to declare.

Role of funding sources

This work was supported by grants from the 3R Research Foundation, Munsingen, Switzerland and the AO Foundation, Davos, Switzerland.

Acknowledgments

We thank Prof U. Zollinger of the Department of Forensic Medicine at the University of Bern, Dr. Eva Shimaoka, Nicole Kaufmann, Prasanna Perumbuli and Elke Berger for assistance. We

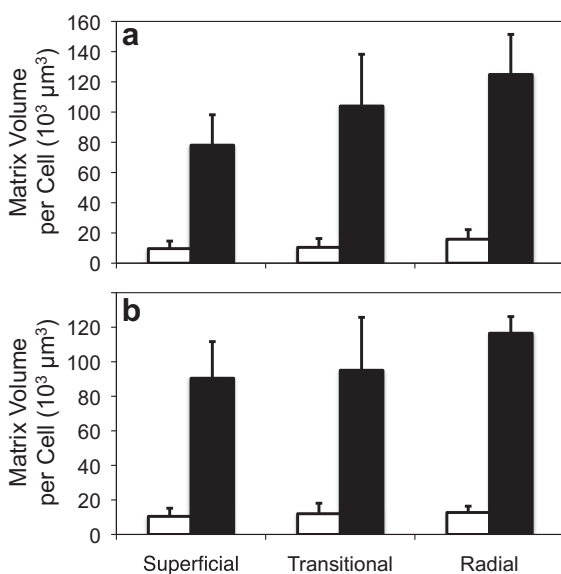


Fig. 5. Pericellular (white bars) and interterritorial (black bars) matrix volume per cell within cartilage from superficial, transitional and radial tissue zones. Data were acquired from a combination of confocal and EM of a) medial tibia not meniscus-covered (MTN; $n = 5$) and b) talus (TAL; $n = 7$) cartilage.

also thank Barbara Krieger from the Institute of Anatomy at the University of Bern for her assistance in digitizing the transmission electron micrographs.

Glossary of Abbreviations

MFC	medial femoral condyle
MTN	medial tibial plateau (not meniscus-covered)
TAL	talus dome
DTB	distal tibia
V_V	chondrocyte volume per unit cartilage volume
S_V	chondrocyte surface area per unit cartilage volume
N_V	number of chondrocytes per unit cartilage volume
N_{Vc}	number of chondrons per unit cartilage volume
V	chondrocyte volume
S	chondrocyte surface area
M	matrix volume per chondrocyte
N_C	number of chondrons per chondron
M_C	matrix volume per chondron
N_{AS}	total number of chondrocytes per unit articular surface
N_{ASc}	total number of chondrons per unit articular surface
P_M	pericellular matrix volume per total matrix volume

Supplementary data

Supplementary data related to this article can be found at <http://dx.doi.org/10.1016/j.joca.2013.09.011>.

References

- Poole AR, Pidoux I, Reiner A, Rosenberg L. An immunoelectron microscope study of the organization of proteoglycan monomer, link protein, and collagen in the matrix of articular cartilage. *J Cell Biol* 1982;93:921–37.
- Hunziker EB, Quinn TM, Hauselmann HJ. Quantitative structural organization of normal adult human articular cartilage. *Osteoarthritis Cartilage* 2002;10:564–72.
- Grodzinsky AJ. Electromechanical and physicochemical properties of connective tissue. *Crit Rev Biomed Eng* 1983;9:133–99.
- Maroudas A. Biophysical chemistry of cartilaginous tissues with special reference to solute and fluid transport. *Biorheology* 1975;12:233–48.
- Vanwanseele B, Lucchinetti E, Stussi E. The effects of immobilization on the characteristics of articular cartilage: current concepts and future directions. *Osteoarthritis Cartilage* 2002;10:408–19.
- Poole AR, Pidoux I, Reiner A, Tang LH, Choi H, Rosenberg L. Localization of proteoglycan monomer and link protein in the matrix of bovine articular cartilage: an immunohistochemical study. *J Histochem Cytochem* 1980;28:621–35.
- Guilak F, Alexopoulos LG, Upton ML, Youn I, Choi JB, Cao L, et al. The pericellular matrix as a transducer of biomechanical and biochemical signals in articular cartilage. *Ann N Y Acad Sci* 2006;1068:498–512.
- Eckstein F, Faber S, Muhlbauer R, Hohe J, Englmeier KH, Reiser M, et al. Functional adaptation of human joints to mechanical stimuli. *Osteoarthritis Cartilage* 2002;10:44–50.
- Huch K, Kuettner KE, Dieppe P. Osteoarthritis in ankle and knee joints. *Semin Arthritis Rheum* 1997;26:667–74.
- Koh J, Dietz J. Osteoarthritis in other joints (hip, elbow, foot, ankle, toes, wrist) after sports injuries. *Clin Sports Med* 2005;24:57–70.
- Kuijt MT, Inklaar H, Gouttebauge V, Frings-Dresen MH. Knee and ankle osteoarthritis in former elite soccer players: a systematic review of the recent literature. *J Sci Med Sport* 2012;15:480–7.
- Kujala UM, Kaprio J, Sarna S. Osteoarthritis of weight bearing joints of lower limbs in former elite male athletes. *BMJ* 1994;308:231–4.
- McDaniel G, Renner JB, Sloane R, Kraus VB. Association of knee and ankle osteoarthritis with physical performance. *Osteoarthritis Cartilage* 2011;19:634–8.
- Talroth K, Harilainen A, Kerttula L, Sayed R. Ankle osteoarthritis is associated with knee osteoarthritis. Conclusions based on mechanical axis radiographs. *Arch Orthop Trauma Surg* 2008;128:555–60.
- Hubbard TJ, Hicks-Little C, Cordova M. Changes in ankle mechanical stability in those with knee osteoarthritis. *Arch Phys Med Rehabil* 2010;91:73–7.
- Astephen JL, Deluzio KJ, Caldwell GE, Dunbar MJ. Biomechanical changes at the hip, knee, and ankle joints during gait are associated with knee osteoarthritis severity. *J Orthop Res* 2008;26:332–41.
- Guler H, Karazincir S, Turhanoglu AD, Sahin G, Balci A, Ozer C. Effect of coexisting foot deformity on disability in women with knee osteoarthritis. *J Am Podiatr Med Assoc* 2009;99:23–7.
- Kerrigan DC, Todd MK, Riley PO. Knee osteoarthritis and high-heeled shoes. *Lancet* 1998;351:1399–401.
- Shepherd DE, Seedhom BB. Thickness of human articular cartilage in joints of the lower limb. *Ann Rheum Dis* 1999;58:27–34.
- Huch K. Knee and ankle: human joints with different susceptibility to osteoarthritis reveal different cartilage cellularity and matrix synthesis in vitro. *Arch Orthop Trauma Surg* 2001;121:301–6.
- Kerin A, Patwari P, Kuettner K, Cole A, Grodzinsky A. Molecular basis of osteoarthritis: biomechanical aspects. *Cell Mol Life Sci* 2002;59:27–35.
- Treppo S, Koepp H, Quan EC, Cole AA, Kuettner KE, Grodzinsky AJ. Comparison of biomechanical and biochemical properties of cartilage from human knee and ankle pairs. *J Orthop Res* 2000;18:739–48.
- Buckwalter JA, Mankin HJ. Articular cartilage: degeneration and osteoarthritis, repair, regeneration, and transplantation. *Instr Course Lect* 1998;47:487–504.
- Hendren L, Beeson P. A review of the differences between normal and osteoarthritis articular cartilage in human knee and ankle joints. *Foot (Edinb)* 2009;19:171–6.
- Runhaar J, Koes BW, Clockaerts S, Bierma-Zeinstra SM. A systematic review on changed biomechanics of lower extremities in obese individuals: a possible role in development of osteoarthritis. *Obes Rev* 2011;12:1071–82.
- Vincent KR, Conrad BP, Fregly BJ, Vincent HK. The pathophysiology of osteoarthritis: a mechanical perspective on the knee joint. *PMR* 2012;4:S3–9.
- Quinn TM, Hunziker EB, Hauselmann HJ. Variation of cell and matrix morphologies in articular cartilage among locations in the adult human knee. *Osteoarthritis Cartilage* 2005;13:672–8.
- Iwaki H, Pinskerova V, Freeman MA. Tibiofemoral movement 1: the shapes and relative movements of the femur and tibia in the unloaded cadaver knee. *J Bone Joint Surg Br* 2000;82:1189–95.
- Bush PG, Hall AC. The volume and morphology of chondrocytes within non-degenerate and degenerate human articular cartilage. *Osteoarthritis Cartilage* 2003;11:242–51.

30. Franz T, Hasler EM, Hagg R, Weiler C, Jakob RP, Mainil-Varlet P. In situ compressive stiffness, biochemical composition, and structural integrity of articular cartilage of the human knee joint. *Osteoarthritis Cartilage* 2001;9:582–92.
31. Froimson MI, Ratcliffe A, Gardner TR, Mow VC. Differences in patellofemoral joint cartilage material properties and their significance to the etiology of cartilage surface fibrillation. *Osteoarthritis Cartilage* 1997;5:377–86.
32. Cruz-Orive LM, Weibel ER. Recent stereological methods for cell biology: a brief survey. *Am J Physiol* 1990;258:L148–56.
33. Gundersen HJ, Bendtsen TF, Korbo L, Marcussen N, Moller A. Some new, simple and efficient stereological methods and their use in pathological research and diagnosis. *APMIS* 1988;96:379–94.
34. Baddeley AJ, Gundersen HJG, Cruz Orive LM. Estimation of surface area from vertical sections. *J Microsc* 1986;142:259–76.
35. Stockwell RA. Cell density, cell size and cartilage thickness in adult mammalian articular cartilage. *J Anat* 1971;108:584–93.
36. Simon WH, Friedenbergs S, Richardson S. Joint congruence. A correlation of joint congruence and thickness of articular cartilage in dogs. *J Bone Joint Surg Am* 1973;55:1614–20.
37. Vanwanseele B, Eckstein F, Knecht H, Stussi E, Spaepen A. Knee cartilage of spinal cord-injured patients displays progressive thinning in the absence of normal joint loading and movement. *Arthritis Rheum* 2002;46:2073–8.
38. Lyyra T, Kiviranta I, Vaatainen U, Helminen HJ, Jurvelin JS. In vivo characterization of indentation stiffness of articular cartilage in the normal human knee. *J Biomed Mater Res* 1999;48:482–7.
39. Wong BL, Kim SH, Antonacci JM, McIlwraith CW, Sah RL. Cartilage shear dynamics during tibio-femoral articulation: effect of acute joint injury and tribosupplementation on synovial fluid lubrication. *Osteoarthritis Cartilage* 2010;18:464–71.
40. Buckley MR, Gleghorn JP, Bonassar LJ, Cohen I. Mapping the depth dependence of shear properties in articular cartilage. *J Biomech* 2008;41:2430–7.
41. Jadin KD, Bae WC, Schumacher BL, Sah RL. Three-dimensional (3-D) imaging of chondrocytes in articular cartilage: growth-associated changes in cell organization. *Biomaterials* 2007;28:230–9.